

Fission and the r -process nucleosynthesis of translead nuclei

Samuel A. Giuliani,^{1,*} Gabriel Martínez-Pinedo,^{2,3,†} Meng-Ru Wu,^{4,5,‡} and Luis M. Robledo^{6,7,§}

¹*Department of Physics and Astronomy and NSCL/FRIB Laboratory,
Michigan State University, East Lansing, Michigan 48824, USA*

²*GSI Helmholtzzentrum für Schwerionenforschung, Planckstraße 1, 64291 Darmstadt, Germany*

³*Institut für Kernphysik (Theoriezentrum), Technische Universität Darmstadt,
Schlossgartenstraße 2, 64298 Darmstadt, Germany*

⁴*Institute of Physics, Academia Sinica, Taipei, 11529, Taiwan*

⁵*Institute of Astronomy and Astrophysics, Academia Sinica, Taipei, 10617, Taiwan*

⁶*Center for Computational Simulation, Universidad Politécnica de Madrid, Campus de Montegancedo, 28660 Madrid, Spain*

⁷*Departamento de Física Teórica, Universidad Autónoma de Madrid, 28049 Madrid, Spain*

(Dated: May 15, 2022)

We study the impact of fission on the production and destruction of translead nuclei during the r -process nucleosynthesis occurring in neutron star mergers. Abundance patterns and rates of nuclear energy production are obtained for different ejecta conditions using two sets of stellar reaction rates, one of which is based on microscopic and consistent calculations of nuclear masses, fission barriers and collective inertias. We show that the accumulation of fissioning material during the r process can strongly affect the free neutron abundance after the r -process freeze-out. This leads to a significant impact on the abundances of heavy nuclei that undergo α decay or spontaneous fission, affecting the radioactive energy production by the ejecta at timescales relevant for kilonova emission.

I. INTRODUCTION

Sixty years after the seminal works of B²FH and Cameron [1, 2], where the rapid neutron capture process (r process) was firstly indicated as the main mechanism responsible for the production of the heaviest elements observed in the universe, the GW170817 gravitational wave signal [3] and its associated AT 2017gfo electromagnetic (EM) counterpart [4] provided the first evidence that r -process nucleosynthesis occurs in neutron star mergers (NSM) [5–8]. This evidence arose from the observed optical and near-infrared emissions, which were found to be consistent with a quasi-thermal transient known as kilonova or macronova powered by the radioactive decay of freshly-synthesized r -process nuclei [9–12]. However, whether NSM are the only astrophysical source of r -process elements in the universe remains an open question [13]. This is because despite the large amount of information extracted from the multimessenger observations, the detailed composition of the ejected material is still unclear. For instance, the near-infrared kilonova emission that was observed at timescale of several days is consistent with predictions assuming a significant presence of lanthanides (mass fraction $\gtrsim 10^{-2}$) in the ejecta [14, 15], but the exact range of the produced nuclei or whether there was a possible presence of heavier elements has not yet been determined. In this context, future observations of late-time ($\gtrsim 10$ days) kilonova light curves showing signatures related to the decay of particular nuclei, together with improved kilonova emission

modeling, would thus provide invaluable information to offer further insights in our understanding of the origin of r -process elements [16–18].

Therefore, both future observations as well as improved theoretical yield predictions are urgently required. From the theoretical nuclear physics side, one aspect that must be addressed is the sensitivity of kilonova light curves with respect to the presence of long-lived heavy nuclei. The presence of Uranium and Thorium in metal-poor stars, as well as in the solar system, indicates that if NSM are a major contributor to the production of r -process nuclei, the r -process path therein must reach the region of actinides. Therefore, it is likely that fission happens during and/or after the r process. Previous studies have shown that the kilonova lightcurves, particularly at late times, can sensitively depend on the produced amount of translead nuclei, e.g., those with mass number A between $222 \leq A \leq 225$ and $A = 254$, depending on the adopted nuclear mass model [17, 19–21], and/or the assumed fission probabilities of heavy nuclei during their decay [16, 22]. However, crucial understanding on the role played by fission in the production and destruction of translead nuclei during and after the r process is still lacking.

In this paper, we study the production of translead nuclei during the r -process nucleosynthesis using two different sets of stellar reaction rates and trajectories representing three different ejecta conditions in NSM. In particular, we focus on the role that fission plays in the destruction of very heavy elements and the implications for the electromagnetic transients powered by the radioactive decay of the synthesized nuclei. The paper is organized as follows: Section II discusses the nuclear properties underlying the stellar reactions rates and the different trajectories employed in this work; Section III reports the main results concerning the evolution of total

* giuliani@nscl.msu.edu

† g.martinez@gsi.de

‡ mwu@gate.sinica.edu.tw

§ luis.robledo@uam.es

abundances and nuclear energy release rates; finally, Section IV summarizes the main findings and outline future works.

II. METHOD

One of the major challenges in r -process nucleosynthesis calculations is to study the impact of nuclear properties in the abundance patterns and kilonova light curves. The difficulties arise from the fact that the nuclear reaction network calculations simulating the r -process nucleosynthesis require the knowledge of nuclear masses, reactions rates and decay properties for several thousands of nuclei placed between the valley of stability and the neutron drip-line. Since most of these nuclei are out-of-reach in the current and next-future experimental facilities, the calculations heavily rely on theoretical predictions of these nuclear properties, bringing a large uncertainty in the nucleosynthesis outcome [23].

Rather critical is the case of fission, where the data provided from experiment and theory suitable for r -process calculations is particularly scarce. As a result, only few papers so far addressed the impact of fission during the r -process nucleosynthesis [22, 24–29]. The aim of this paper is then to improve the understanding of the role played by fission in the production of translead nuclei and its possible relevance for kilonova by employing a recently developed set of reaction rates and fission properties based on the Barcelona-Catania-Paris-Madrid (BCPM) energy density functional (EDF) [30, 31].

The BCPM neutron-induced reaction rates, α -decay rates and spontaneous fission lifetimes were obtained using the nuclear masses, fission barriers and collective inertias predicted by the BCPM EDF [32]. This is one of the few attempts to derive a set of reaction rates and nuclear decay properties suited for r -process calculations from a consistent nuclear input (see also Ref. [22, 25]). Since β -decay rates are not available for this functional we employed the finite range droplet model (FRDM) β -decay rates [33] and derived a set of β -delayed fission rates based on BCPM fission barriers and an estimate of the FRDM beta strength function from the neutron emission probabilities. For nuclei with $Z < 84$, where fission is not expected to play a relevant role, we use the neutron capture rates based on the FRDM masses [34] as detailed in Ref. [19]. Previous r -process calculations involving fission have often used reaction rates from Ref. [35], which are based on a combination of FRDM nuclear masses [36] and Thomas-Fermi (TF) fission barriers [37] (see e.g. Ref. [19, 27]). In this work we refer to such combination as FRDM+TF and consider it as our reference model.

Fig. 1 shows the BCPM and FRDM+TF predictions of the highest fission barrier (B_f), the difference between fission barrier and β -decay Q -value ($B_f - Q_\beta$) [38] and the difference between fission barrier and neutron separation energy ($B_f - S_n$) for nuclei with $Z \geq 84$. These quantities provide a rough estimation of the stability of each

nucleus against the different fission modes: spontaneous fission, β -delayed fission and neutron-induced fission, respectively. Evidently, the smaller these values are, the larger the fission probabilities become. Looking at nuclei close to the neutron dripline, it is possible to conclude that BCPM predicts systematically larger fission barriers compared to TF, particularly in the vicinity of the $N = 184$ shell closure. In Section III we will show how these properties, fission barriers, neutron separation energies and Q_β values, determine the amount of material that can be accumulated in the heaviest region of the r -process nucleosynthesis.

Regarding the astrophysical scenario, we focused our study in the r -process nucleosynthesis occurring in NSM. In order to cover different astrophysical conditions, we employed three trajectories representing different kind of ejecta conditions. The evolution of their mass density, temperature, entropy, and the free neutron number density n_n are plotted in Fig. 2. The ones labeled by (dynamical) “hot” and (dynamical) “cold” are trajectories produced by general-relativistic merger simulation [39] that were used in previous studies discussing the role of fission in shaping the r -process abundances [19]. Both of them have initially low entropies of $\sim 1 k_B$ per nucleon and very low electron fraction per nucleon $Y_e \lesssim 0.05$. The difference between them is that the dynamical “hot” ejecta expand slower when compared to the dynamical “cold” one. Therefore, the nuclear energy release during the r process is able to reheat the temperature to $\gtrsim 1$ GK for the former, but only ~ 0.2 GK for the latter (see Fig. 1 and Eq. [8] in Ref. [19]). Consequently, an $(n, \gamma) \rightleftharpoons (\gamma, n)$ equilibrium between the neutron-capture rates and the reverse photo-dissociation rates is only achieved for the former, but not the latter. As for the trajectory labeled by disk, it is parametrized in the same way as in Ref. [40], with an early-time expansion timescale $\tau = 10$ ms, initial entropy $s = 10 k_B$ per nucleon, and initial $Y_e = 0.15$. This trajectory mimics the neutron-rich condition found in viscous outflows from the post-merger accretion disk [41–43].

Fig. 3 shows the r -process abundances predicted by FRDM+TF and BCPM at the time of 1 Gyr for these three different ejecta conditions. All the abundances reproduce the main features of the “strong” r -process pattern, where elements from the second peak up to actinides have been synthesized. Nevertheless, substantial differences between the predicted abundances are observed that will be discussed in the next section.

III. RESULTS

A. Impact of fission on abundances pattern

Fig. 4 shows the r -process abundances of nuclei beyond $A = 180$ predicted by FRDM+TF and BCPM in each scenario at four different stages of the evolution: at freeze-out, defined as the moment when the neutron-to-

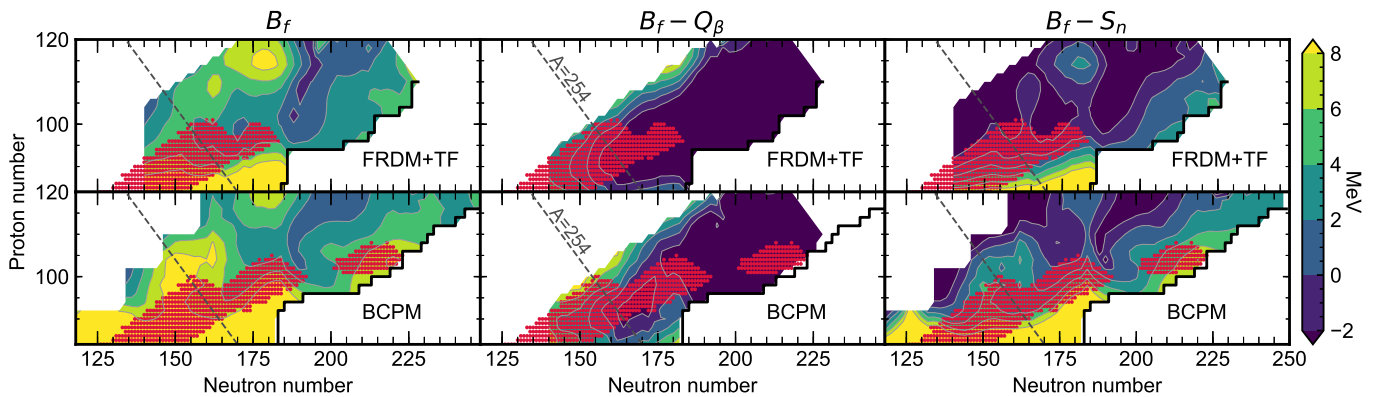


FIG. 1. Highest fission barrier (B_f), and energy windows for beta-delayed fission ($B_f - Q_\beta$) and neutron-induced fission ($B_f - S_n$) predicted by FRDM+TF (upper panels) and BCPM (lower panels) as a function of proton and neutron number. B_f and S_n values correspond to the nucleus with Z protons and N neutrons, while Q_β values correspond to the FRDM prediction for the $(Z - 1, N + 1)$ parental nucleus. All the quantities are in MeV. Red circles indicate the r -process nuclei produced at $t \sim 10$ s in the hot dynamical ejecta nucleosynthesis.

seed ratio $n/s = 1$ (where “seed” includes all nuclei heavier than ${}^4\text{He}$); at the moment when the average timescale for neutron captures $\tau_{(n,\gamma)}$ equals the average timescale for β decays τ_β ; at 1 day, which is taken as a timescale indicative for kilonova observations; and the final abundances calculated at 1 Gyr.

For the hot and cold dynamical ejecta the abundances predicted by FRDM+TF and BCPM visibly differ already at freeze-out. In particular, FRDM+TF shows a peak at $A \sim 260$ which is absent in BCPM, while the latter predict a large accumulation of material around $A \sim 280$. By comparing the nuclear properties of the two models, we found that a combination of several factors contribute to determine these variations. Firstly, differences in the predicted neutron separation energies (and, consequently, in shell gap energies) can entail accumulation of material at different mass numbers, particularly during the initial stages of the evolution. Secondly, changes in the fission barriers modify the survival probability of nuclei and determine the end of the r -process path. Ultimately, the impact of these variations on the r -process abundances is driven by the β -decay rates, which regulate the speed flow of the r -process material. In the case of the abundances plotted in Fig. 4, FRDM predicts a strong shell gap at $N = 172$, which results in the abundances peak at $A \sim 260$. Conversely, the larger fission barriers and shell gap predicted by BCPM at $N = 184$ [32] are responsible for the larger accumulation of material at $A \sim 280$. These variations are also visible in Fig. 5, where the r -process path at freeze-out predicted by BCPM and FRDM+TF for the hot dynamical trajectory is depicted. At $N = 184$, the r -process path obtained with BCPM model can substantially populate nuclei up to ${}^{280}_{96}\text{Cm}$ ($t_{1/2} = 84$ ms, according to the beta-decay half-life predictions of Ref. [33]), while the FRDM+TF r -process path accumulates material mostly around ${}^{278}_{94}\text{Pu}$ ($t_{1/2} = 32$ ms). At later times nuclei

around $A = 280$ decay via fission, enhancing the abundances above the second peak (see Fig. 3), while the free neutrons emitted by fission fragments produce a shift of the third peak towards larger mass number [27] (see discussion in Ref. [19] regarding the fission fragments distributions used in this work).

Fig. 3 also shows that in the case of the accretion disk FRDM+TF and BCPM predict a very similar final pattern, mainly because of the comparable amount of material accumulated at $A \sim 280$. The conditions in this trajectory are less neutron rich than in the dynamical ones: For instance, the initial neutron-to-seed ratio is $n/s \sim 120$, compared to $n/s \sim 600$ and $n/s \sim 1200$ of the hot and cold dynamical ejecta, respectively. These conditions do not allow the r process to efficiently overcome the $N = 184$ shell closure, since the number of free neutrons is mostly depleted when the material reaches the $A \sim 280$ region.

One can distinguish between two different effects produced by fission in the r -process nucleosynthesis: a direct effect, mainly related to the change in the abundances due to the splitting of the fissioning nuclei; and an indirect effect, induced by the neutron emission of fission fragments (and the subsequent neutron captures). As an example of the latter, Fig. 2 shows that the larger amount of fissioning nuclei predicted by BCPM significantly increases the free neutron densities of the environment after the r -process freeze-out. In the following two sections, we will discuss how these effects impact the rate of energy production at timescales that are relevant for the observation of kilonovae.

B. Fission and the destruction of $A \gtrsim 250$ nuclei

One feature in all the results shown in Fig. 4 is the drastic drop of the abundances for nuclei with $A \gtrsim 250$

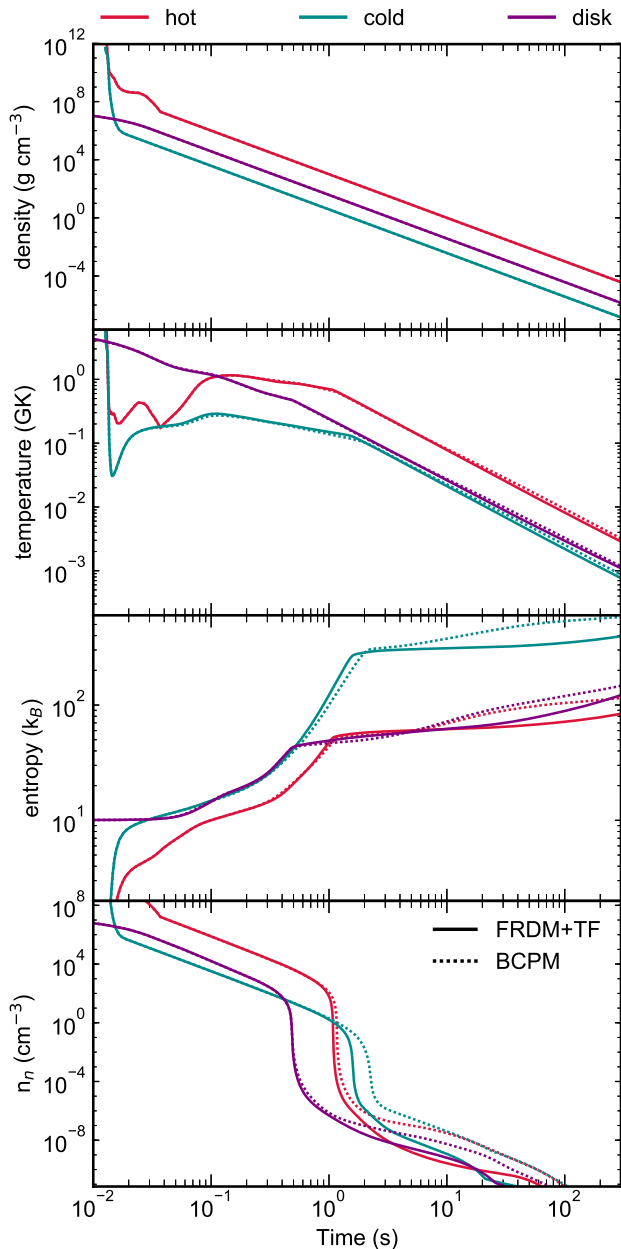


FIG. 2. Evolution of the different thermodynamic variables (from top to bottom): mass density, temperature, entropy and free neutron number density n_n . The different curves represent the predictions obtained with BCPM (dotted lines) and FRDM+TF (solid lines) for three different trajectories: dynamical hot (red curves), dynamical cold (blue curves) and accretion disk (purple curves) (see text for details).

at the time of a day. This has important consequences in terms of kilonova observation, since the decay by spontaneous fission of ^{254}Cf , $t_{1/2} = 60.5 \pm 0.2$ days [44], can sensibly impact the shape and magnitude of the kilonova lightcurves at $t \gtrsim 100$ days [16, 17]. Therefore, it is important to understand the mechanisms that are responsible for the destruction of these nuclei as they also determine the amount of ^{254}Cf that survives at kilonova

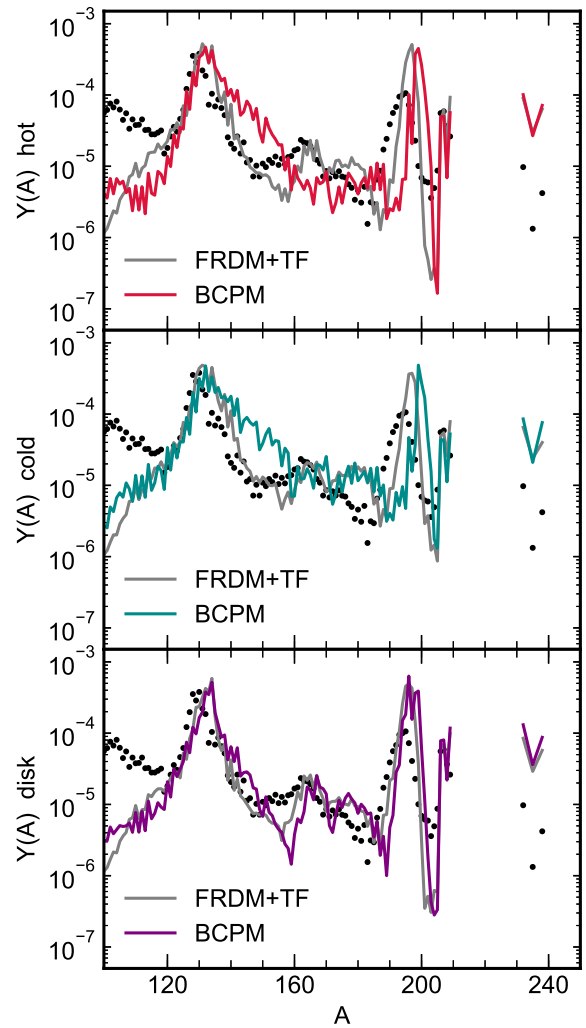


FIG. 3. Abundances as a function of mass number predicted by BCPM and FRDM+TF at 1 Gyr for the three different ejecta conditions: dynamical hot (upper panel), dynamical cold (middle panel) and accretion disk (lower panel). As a reference, black dots show the renormalized solar r -process abundances.

times. For this purpose, we performed additional calculations by switching off different fission channels (neutron-induced, β -delayed and spontaneous fission) and compare the impact of each channel on the remaining abundance of $A \gtrsim 250$ nuclei at 1 day. While we only focus on the results obtained in the hot dynamical case below, we note that similar outcomes were obtained in the cold and accretion scenarios.

The upper panels in Fig. 6 show the abundances predicted with FRDM+TF (left panel) and BCPM (right panel) when different fission channels are turned off. For spontaneous and β -delayed fission, we suppressed the channel from the beginning of the simulation, while neutron-induced fission was turned off only after the freeze-out. We point out that only theoretical rates have been switched off. We find that within each set of reac-

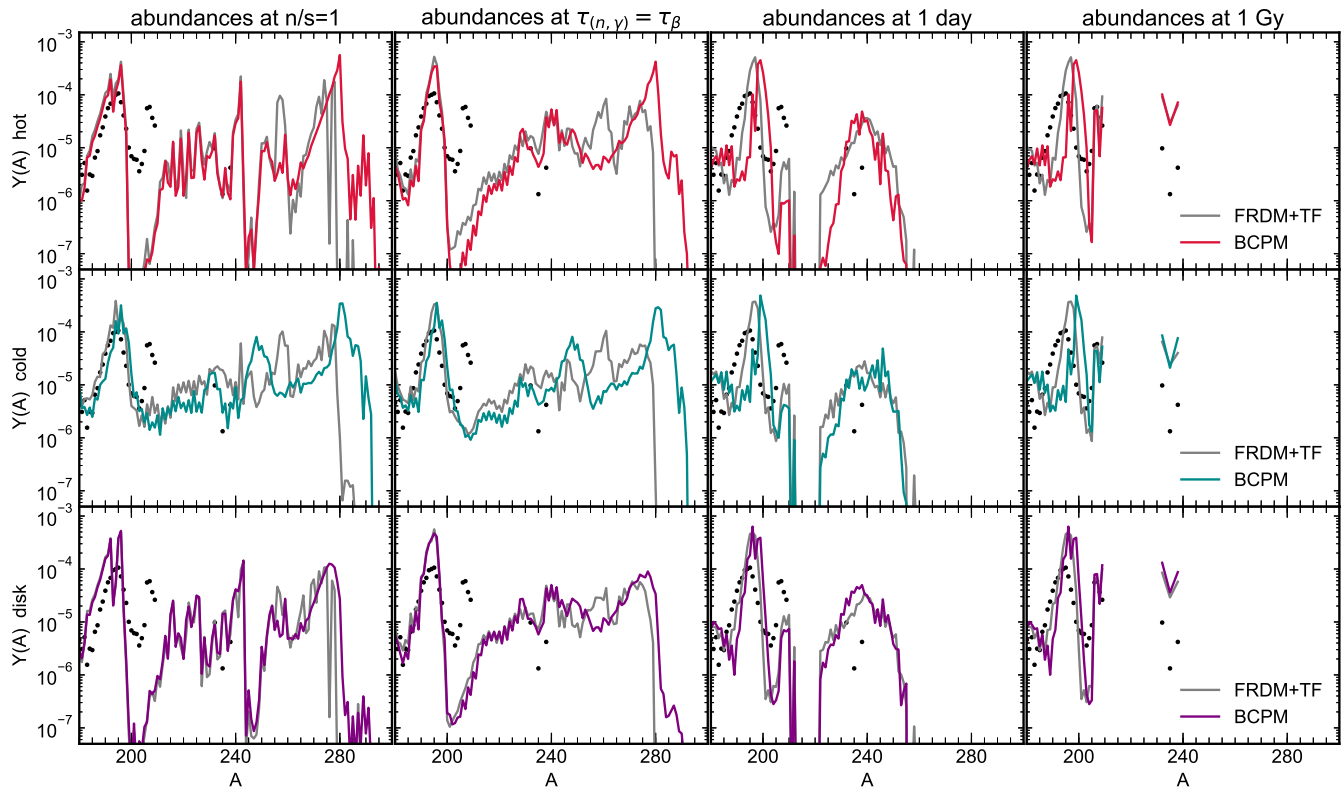


FIG. 4. Abundances as a function of mass number predicted by FRDM+TF and BCPM at four different times. Each row represent a different type of ejecta: dynamical hot (upper panels), dynamical cold (middle panels) and accretion disk (lower panels). Black dots represent solar r -process abundances, which are renormalized by the same factor in all plots.

tion rates, the sharp drop of abundances at $A \gtrsim 250$ remains, suggesting that all the fission channels contribute to the destruction for $A \gtrsim 250$ nuclei.

The reason behind this destruction can be understood by comparing the abundance distribution after the r -process freeze-out to the fission barriers shown in Fig. 1. Nuclei that are present at $t \sim 10$ s in the hot dynamical ejecta scenario are plotted as solid symbols. Left panels shows that the abundance distributions closely follows contour lines of constant fission barrier height, and that none of the two models predict the synthesis of nuclei with $B_f < 2$ MeV that can be populated. We conclude therefore that the reason for such efficient destruction mechanism of all the fission channels is related to the presence of low fission barriers, which in turn make nuclei unstable against fission decay regardless of the mechanism forming those nuclei. The only calculation where nuclei with $A > 250$ survive at 1 day is in the BCPM model without spontaneous fission. In this case, the larger $B_f - Q_\beta$ predicted by BCPM around $N = 184$ allow part of the material to undergo multiple β decays before entering in the region of low B_f and fission.

One should notice that in Fig. 1 there are nuclei with a negative energy window for β -delayed fission ($B_f - Q_\beta$) that are populated. The reason for this is twofold: Firstly, the β -decay proceeds mainly via states with low

excitation energy, hence it is the magnitude of the barrier and not necessarily $B_f - Q_\beta$ that determines the fission survival probability after beta-decay. Secondly, nuclei populated in Fig. 1 have $S_n < B_f$, as evinced by the right panels in the same plot, which favors the emissions of neutrons over a possible fission decay.

Bottom panels in Fig. 6 show the total $A = 254$ abundance predicted in the hot dynamical ejecta using BCPM and FRDM+TF. From these plots it is possible to conclude that neutron-induced fission is responsible for the destruction of $A = 254$ isobars in both cases. This destruction channel is particularly efficient in the case with the BCPM model, at the time of 0.4–2.0 seconds, due to the fact that the neutron number density after the r -process freeze-out is up to four orders of magnitude larger than that with the FRDM+TF model (see the bottom panel in Fig. 2). Actually the destruction of $A = 254$ isobars should be considered as a more general feature, where the destruction rate of nuclei post freeze-out is strongly related to variations in the neutron number density since this directly determines the neutron captures and neutron-induced fission rates. On the other hand, β -delayed fission only operates to destruct the $A = 254$ isobars at later times with FRDM+TF model, since the large $B_f - Q_\beta$ predicted by BCPM disfavour this fission channel (see middle panels in Fig 1).

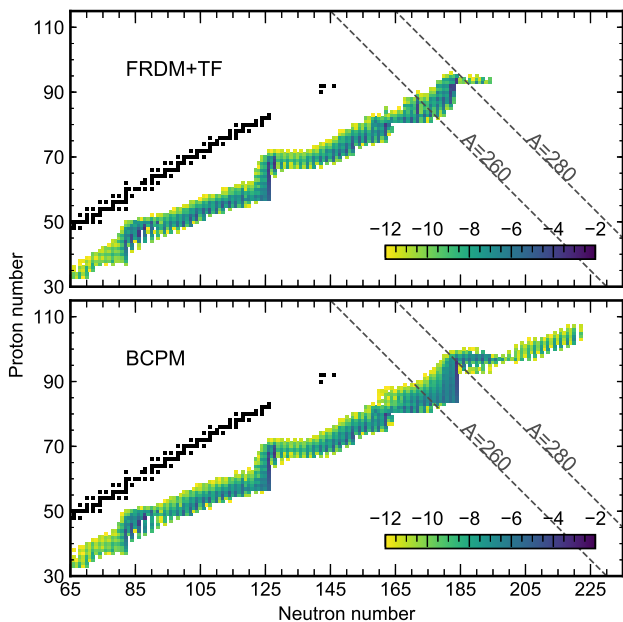


FIG. 5. Abundances (in log scale) at freeze-out predicted by FRDM+TF (upper panel) and BCPM (lower plot) in the hot dynamical ejecta. Black squares represent stable nuclei.

Fig. 7 shows the nuclear energy release rate produced by fission, β and α decays as a function of time obtained with both models for the different ejecta conditions. The “bump” feature at $t \sim 128$ days, for curves associated with fission, is driven by the spontaneous fission decay of ^{254}Cf . They clearly show that the released nuclear energy can be comparable to those from β -decays in all cases with FRDM+TF model, while being much smaller for cases with the BCPM models, especially for the hot and cold trajectories, whose free neutron number densities are much higher after the freeze-out (see Fig. 2). We conclude, therefore, that more ^{254}Cf is accumulated when the amount of material in the $A \sim 280$ fissioning region is smaller. One can also infer this by noticing that the models with the smallest energy production by fission in Fig. 7 are those showing the largest “fissioning peak” in Fig. 4. We found that between 0.4 and 1.2 seconds, the average number of neutrons released by fission with BCPM is between three and six units larger than FRDM+TF in both dynamical scenarios (while in the disk ejecta the difference decreases quickly to zero). These free neutrons released after the freeze-out generate new neutron-induced fission events, in a self-sustained mechanism similar to the one occurring in nuclear reactors, destroying the progenitors of the ^{254}Cf as shown in Fig. 6.

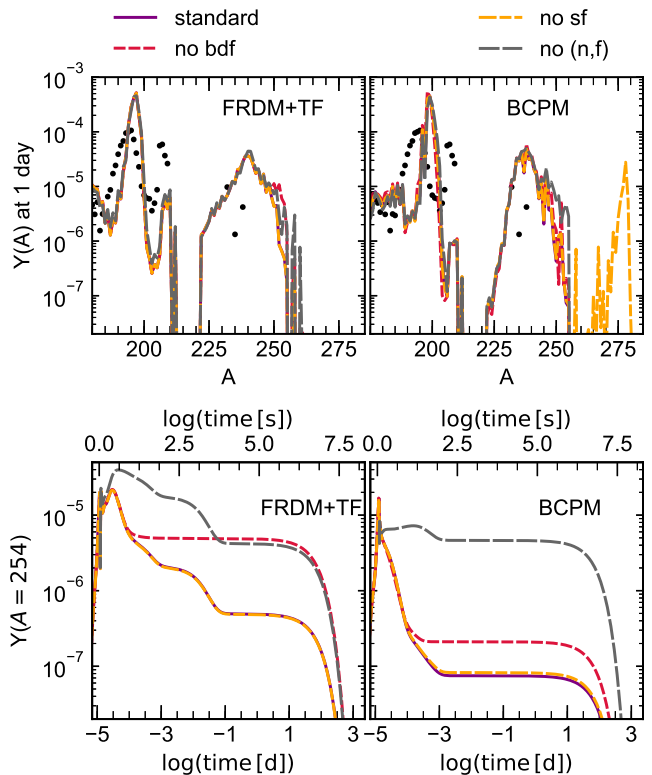


FIG. 6. Impact of single fission channels on the abundances of nuclei with $A \gtrsim 250$ at 1 day (top panels) and on the evolution of $A = 254$ abundances (bottom panels) for the hot dynamical ejecta. The different curves show the abundances predicted when different fission channels are suppressed: β -delayed fission (*bdf*, red dashed line), spontaneous fission (*sf*, yellow dashed line) and neutron induced fission (*(n, f)*, grey dashed line). The purple solid line corresponds to standard calculations, when all the fission are included. Left and right panels correspond to FRDM+TF and BCPM, respectively.

C. Impact of fission on abundance of nuclei with $A = 222 - 225$

In addition to the impact on the heating from the spontaneous fission of ^{254}Cf , Fig. 7 also shows that calculations with the BCPM model predict reduced nuclear energy release rates from α -decays, that is powered by the decay chains of nuclei with $222 \leq A \leq 225$ during the relevant kilonova timescale of 3–100 days [17]. This can be clearly seen by comparing the abundances of these nuclei shown in Fig. 4 at the time of a day for all cases with the BCPM model to those with the FRDM+TF model, which shows that BCPM predicts lower abundances of nuclei with $220 \leq A \leq 230$, particularly in the case of dynamical and cold ejecta.

On the other hand, the same plot shows that the BCPM model generally predicts larger amount of nuclei between $230 \leq A \leq 240$. Combining this with the fact that the final abundances in the lead peak ($A \sim 208$) and those of uranium and thorium predicted by BCPM

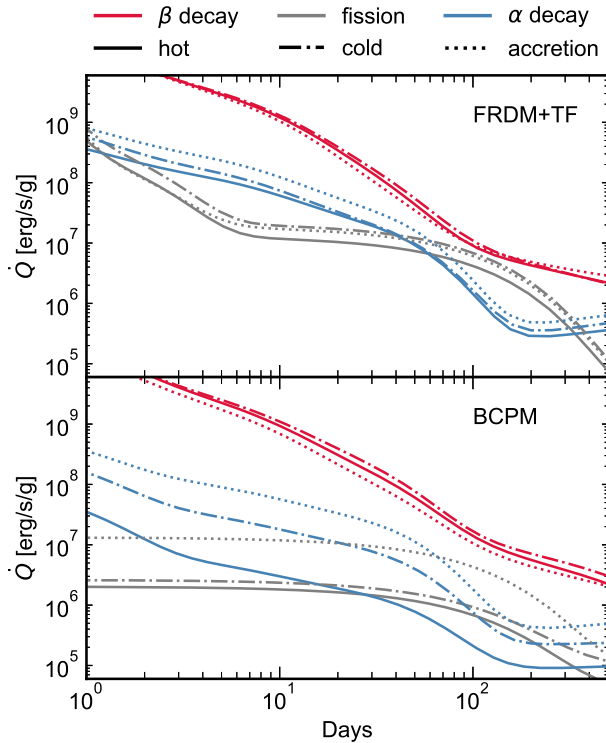


FIG. 7. Radioactive energy emitted by β decay (grey lines), α decay (blue lines) and fission (red lines) as a function of time for different ejecta conditions: dynamical hot (solid lines), dynamical cold (dash-dotted lines) and accretion disk (dotted lines). The upper panel and lower panel show the results predicted by FRDM+TF and BCPM, respectively.

and FRDM+TF are very similar, it indicates that the amount of material with $A \geq 220$ produced at 1 day is in fact similar in both BCPM and FRDM+TF calculations. The reduced abundances of $220 \leq A \leq 230$ at a day with the BCPM model can once again be connected with the larger amount of free neutrons after the r -process freeze-out. Neutron captures on these nuclei after the freeze-out moves the material towards higher mass numbers. Fig. 8 shows the time evolution of the total abundances of nuclei with $220 \leq A \leq 230$. The strong decrease for cases with the BCPM model between $1.2 \text{ s} \lesssim t \lesssim 3 \text{ s}$ provide clear evidence that these nuclei are being transported toward larger mass numbers.

Finally, Fig. 9 shows the time evolution of the ejecta heating rate Q_{hr} , which mimics the bolometric luminosity of the kilonova at $t \gtrsim$ days post the lightcurve peak. The calculations were performed as described in Ref. [17], which include thermalization corrections, assuming an ejecta mass $M_{ej} = 0.04 M_{\odot}$ with an expanding velocity $v_{ej} = 0.1 c$. The impact of the ^{254}Cf is clearly noticeable at $t \sim 100$ days, where the predictions obtained with FRDM+TF and BCPM visibly differ. In the dynamical scenarios, the larger amount of ^{254}Cf predicted with FRDM+TF [$Y(^{254}\text{Cf}) \approx 4.9 \times 10^{-7}$] results in a heating rate which is three times larger than the one predicted

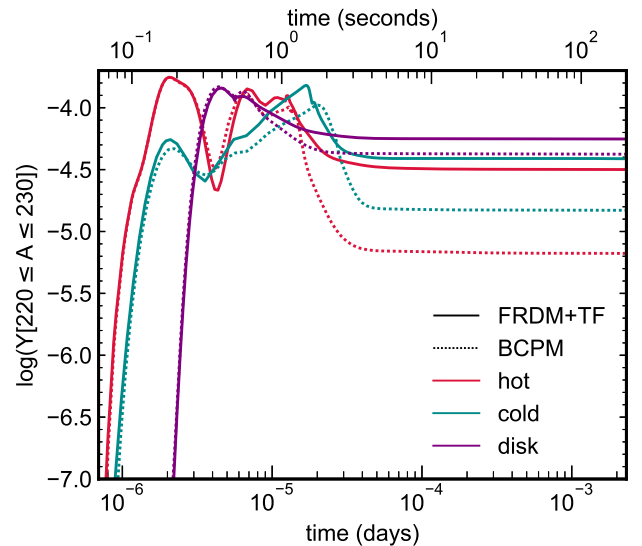


FIG. 8. Evolution of the total $220 \leq A \leq 230$ abundance predicted by FRDM+TF (solid lines) and BCPM (dotted lines) for different trajectories.

using the BCPM model [$Y(^{254}\text{Cf}) \approx 7.4 \times 10^{-8}$]. This result confirms the high sensitivity of kilonova light curve to the amount of ^{254}Cf fissioning at timescales relevant for astronomical observations [16, 17]. We also note that despite the abundances of nuclei with $135 \lesssim A \lesssim 200$ are largely affected by the direct impact of fission, the β -decay heating rate at earlier times are only affected by $\lesssim 50\%$, due to the fact that independently of the fission yields used the produced nuclei have β -decay half-lives within a factor of two.

Finally, the similar abundances of U and Th predicted by BCPM and FRDM+TF indicates that the progenitors of these nuclei have the same nuclear properties in both calculations. This implicitly suggests that the progenitors of late translead elements during the r process are nuclei with $Z < 84$, since BCPM and FRDM+TF calculations only differ in the rates used for nuclei with $Z \geq 84$. It is, therefore, possible to conclude that most the material with $Z \geq 84$ created during the r -process nucleosynthesis fissions.

IV. CONCLUSIONS

We explored the impact of fission on the r -process nucleosynthesis yields in neutron star mergers and the associated nuclear energy release rates relevant for kilonovae. We used two different sets of stellar reaction rates, one of which was recently developed using consistent nuclear energy density functional calculations of nuclear masses, fission barriers and collective inertias [32]. Our calculations show that for the most neutron rich conditions, like those found in the dynamical ejecta, the stability against fission of nuclei around the neutron shell clo-

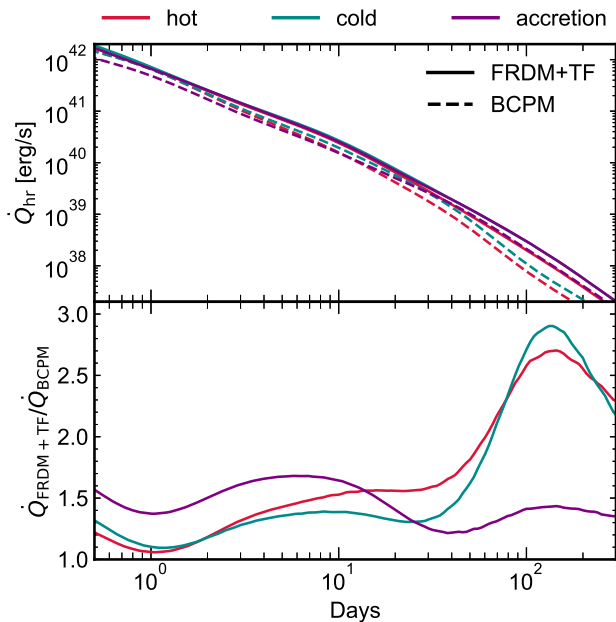


FIG. 9. Upper panel: Ejecta heating rate as a function of time predicted with BCPM (dash-dotted lines) and FRDM+TF (solid lines) for different scenarios. Lower panel: Evolution of the ratio between ejecta heating rates.

sure $N = 184$ is crucial for the build-up of fissioning material during the r process. The fission of these material after the r -process freeze-out can release a large amount of neutrons and significantly alter the free neutrons number density of the ejecta around $1 \text{ s} \lesssim t \lesssim 10 \text{ s}$. Consequently, the neutron-induced fission and neutron-captures associated with these free neutrons can have strong impact on the abundances of nuclei in the mass

number region $A = 220 - 260$, including the α -decaying nuclei with $222 \leq A \leq 225$ and the ^{254}Cf which undergoes spontaneous fission, affecting the ejecta heating rates on timescales relevant for kilonova light curve predictions.

In conclusion, we find an inverse correlation between the amount of material produced around $A = 280$ and the amount of ^{254}Cf produced. This result suggests that future detection or non-detection of ^{254}Cf on kilonova light curves may help to constraint the yields of nuclei around $A \sim 280$ and learn about the nuclear properties in a region that in the foreseeable future will not be experimentally accessed.

ACKNOWLEDGMENTS

SAG would like to thank M. Eichler and N. Vassh for useful discussions. SAG acknowledges support from the U.S. Department of Energy under Award Number DOE-DE-NA0002847 (NNSA, the Stewardship Science Academic Alliances program). The work of GMP is partly supported by the Deutsche Forschungsgemeinschaft (DFG, German Research Foundation) - Projektnummer 279384907 - SFB 1245. MRW acknowledges support from the Ministry of Science and Technology, Taiwan under Grant No. 107-2119-M-001-038. The work of LMR is partly supported by the Spanish grant Nos FIS2015-63770 MINECO and FPA2015-65929 MINECO. SAG and MRW thank the Yukawa Institute for Theoretical Physics in Kyoto for support in the framework of the YITP-T-18-06 workshop, during which several aspects of this work have been discussed. Computations were partly performed on the LOEWE-CSC computer managed by Center for Scientific Computing of the Goethe University Frankfurt.

-
- [1] E. M. Burbidge, G. R. Burbidge, W. A. Fowler, and F. Hoyle, “Synthesis of the Elements in Stars,” *Rev. Mod. Phys.* **29**, 547–650 (1957).
 - [2] A. G. W. Cameron, “Nuclear Reactions in Stars and Nucleogenesis,” *Publ. Astron. Soc. Pac.* **69**, 201 (1957).
 - [3] B. P. Abbott *et al.* (LIGO Scientific Collaboration and Virgo Collaboration), “GW170817: Observation of gravitational waves from a binary neutron star inspiral,” *Phys. Rev. Lett.* **119**, 161101 (2017).
 - [4] B. P. Abbott *et al.*, “Multi-messenger Observations of a Binary Neutron Star Merger,” *Astrophys. J.* **848**, L12 (2017).
 - [5] J. M. Lattimer and David N. Schramm, “Black-hole-neutron-star collisions,” *Astrophys. J.* **192**, L145 (1974).
 - [6] J. M. Lattimer and David N. Schramm, “The tidal disruption of neutron stars by black holes in close binaries,” *Astrophys. J.* **210**, 549 (1976).
 - [7] E. Symbalisty and David N. Schramm, “Neutron star collisions and the r -process,” *Astrophys. Lett.* **22**, 143–145 (1982).
 - [8] C. Freiburghaus, S. Rosswog, and F.-K. Thielemann, “ r -Process in Neutron Star Mergers,” *Astrophys. J.* **525**, L121–L124 (1999).
 - [9] Li-Xin Li and Bohdan Paczyński, “Transient Events from Neutron Star Mergers,” *Astrophys. J.* **507**, L59–L62 (1998).
 - [10] B. D. Metzger, G. Martínez-Pinedo, S. Darbha, E. Quataert, Almudena Arcones, D. Kasen, R. Thomas, P. Nugent, I. V. Panov, and N. T. Zinner, “Electromagnetic counterparts of compact object mergers powered by the radioactive decay of r -process nuclei,” *Mon. Notices Royal Astron. Soc.* **406**, 2650–2662 (2010).
 - [11] L. F. Roberts, D. Kasen, W. H. Lee, and E. Ramirez-Ruiz, “Electromagnetic Transients Powered by Nuclear Decay in the Tidal Tails of Coalescing Compact Binaries,” *Astrophys. J.* **736**, L21 (2011).
 - [12] Stéphane Goriely, Stéphane Hilaire, A. J. Koning, and R. Capote, “Towards Improved Evaluation of Neutron-Induced Fission Cross Section,” *J. Korean Phy. Soc.* **59**, 979 (2011).

- [13] John J. Cowan, Christopher Sneden, James E. Lawler, Ani Aprahamian, Michael Wiescher, Karlheinz Langanke, Gabriel Martínez-Pinedo, and Friedrich-Karl Thielemann, “Making the Heaviest Elements in the Universe: A Review of the Rapid Neutron Capture Process,” arXiv e-prints (2019).
- [14] Daniel Kasen, B. D. Metzger, Jennifer Barnes, Eliot Quataert, and Enrico Ramirez-Ruiz, “Origin of the heavy elements in binary neutron-star mergers from a gravitational-wave event,” *Nature (London)* **551**, 80–84 (2017).
- [15] Kyohei Kawaguchi, Masaru Shibata, and Masaomi Tanaka, “Radiative transfer simulation for the optical and near-infrared electromagnetic counterparts to GW170817,” *Astrophys. J.* **865**, L21 (2018).
- [16] Yong-Lin Zhu, Ryan T. Wollaeger, Nicole Vassh, Rebecca Surman, Trevor M. Sprouse, Matthew R. Mumpower, Peter Möller, G. C. McLaughlin, Oleg Korobkin, Toshihiko Kawano, P. J. Jaffke, Erika M. Holmbeck, C. L. Fryer, W. P. Even, A. J. Couture, and Jennifer Barnes, “Californium-254 and Kilonova Light Curves,” *Astrophys. J.* **863**, L23 (2018).
- [17] Meng-Ru Wu, J. Barnes, G. Martínez-Pinedo, and B. D. Metzger, “Fingerprints of heavy-element nucleosynthesis in the late-time lightcurves of kilonovae,” *Phys. Rev. Lett.* **122**, 062701 (2019).
- [18] Mansi M. Kasliwal, Daniel Kasen, Ryan M. Lau, Daniel A. Perley, Stephan Rosswog, Eran O. Ofek, Kenta Hotokezaka, Ranga-Ram Chary, Jesper Sollerman, Ariel Goobar, and David L. Kaplan, “Spitzer Mid-Infrared Detections of Neutron Star Merger GW170817 Suggests Synthesis of the Heaviest Elements,” *Mon. Notices Royal Astron. Soc.*, L14 (2019).
- [19] Joel de Jesús Mendoza-Temis, Meng-Ru Wu, Karlheinz Langanke, Gabriel Martínez-Pinedo, Andreas Bauswein, and Hans-Thomas Janka, “Nuclear robustness of the r process in neutron-star mergers,” *Phys. Rev. C* **92**, 055805 (2015).
- [20] Jennifer Barnes, Daniel Kasen, Meng-Ru Wu, and Gabriel Martínez-Pinedo, “Radioactivity and thermalization in the ejecta of compact object mergers and their impact on kilonova light curves,” *Astrophys. J.* **829**, 110 (2016).
- [21] Stephan Rosswog, U. Feindt, Oleg Korobkin, Meng-Ru Wu, J. Sollerman, A. Goobar, and Gabriel Martínez-Pinedo, “Detectability of compact binary merger macronovae,” *Class. Quantum Gravity* **34**, 104001 (2017).
- [22] Nicole Vassh, Ramona Vogt, Rebecca Surman, Jorgen Randrup, Trevor Sprouse, Matthew Mumpower, Patrick Jaffke, David Shaw, Erika Holmbeck, Yonglin Zhu, and Gail McLaughlin, “Using excitation-energy dependent fission yields to identify key fissioning nuclei in r-process nucleosynthesis,” (2018).
- [23] Matthew R. Mumpower, Rebecca Surman, G. C. McLaughlin, and A. Aprahamian, “The impact of individual nuclear properties on r-process nucleosynthesis,” *Prog. Part. Nucl. Phys.* **86**, 86–126 (2016).
- [24] I. Petermann, K. Langanke, Gabriel Martínez-Pinedo, I. V. Panov, Paul-Gerhard Reinhard, and F.-K. Thielemann, “Have superheavy elements been produced in nature?” *Eur. Phys. J. A* **48**, 122 (2012).
- [25] Stéphane Goriely, “The fundamental role of fission during r-process nucleosynthesis in neutron star mergers,” *Eur. Phys. J. A* **51**, 22 (2015).
- [26] S. Goriely and G. Martínez-Pinedo, “The production of transuranium elements by the r-process nucleosynthesis,” *Nucl. Phys. A* **944**, 158–176 (2015).
- [27] Marius Eichler, Almudena Arcones, A. Kelić-Heil, Oleg Korobkin, K. Langanke, T. Marketin, Gabriel Martínez-Pinedo, I. V. Panov, T. Rauscher, S. Rosswog, C. Winteler, N. T. Zinner, and F.-K. Thielemann, “The role of fission in neutron star mergers and its impact on the r-process peaks,” *Astrophys. J.* **808**, 30 (2015).
- [28] M. R. Mumpower, T. Kawano, T. M. Sprouse, N. Vassh, E. M. Holmbeck, R. Surman, and P. Möller, “ β -delayed Fission in r-process Nucleosynthesis,” *Astrophys. J.* **869**, 14 (2018).
- [29] Erika M. Holmbeck, Trevor M. Sprouse, Matthew R. Mumpower, Nicole Vassh, Rebecca Surman, Timothy C. Beers, and Toshihiko Kawano, “Actinide Production in the Neutron-rich Ejecta of a Neutron Star Merger,” *Astrophys. J.* **870**, 23 (2019).
- [30] Marcello Baldo, Luis M. Robledo, Peter Schuck, and Xavier Viñas, “New Kohn-Sham density functional based on microscopic nuclear and neutron matter equations of state,” *Phys. Rev. C* **87**, 064305 (2013).
- [31] Samuel A. Giuliani and Luis M. Robledo, “Fission properties of the Barcelona-Catania-Paris-Madrid energy density functional,” *Phys. Rev. C* **88**, 054325 (2013).
- [32] Samuel A. Giuliani, Gabriel Martínez-Pinedo, and Luis M. Robledo, “Fission properties of superheavy nuclei for r-process calculations,” *Phys. Rev. C* **97**, 034323 (2018).
- [33] Peter Möller, B. Pfeiffer, and K.-L. Kratz, “New calculations of gross β -decay properties for astrophysical applications: Speeding-up the classical r process,” *Phys. Rev. C* **67**, 055802 (2003).
- [34] T. Rauscher and F.-K. Thielemann, “Astrophysical Reaction Rates From Statistical Model Calculations,” *At. Data. Nucl. Data Tables* **75**, 1–351 (2000).
- [35] I. V. Panov, I. Yu. Korneev, T. Rauscher, Gabriel Martínez-Pinedo, A. Kelić-Heil, N. T. Zinner, and F.-K. Thielemann, “Neutron-induced astrophysical reaction rates for translead nuclei,” *Astron. Astrophys.* **513**, A61 (2010).
- [36] Peter Möller, J. R. Nix, W. D. Myers, and W. J. Świątecki, “Nuclear Ground-State Masses and Deformations,” *At. Data. Nucl. Data Tables* **59**, 185–381 (1995).
- [37] W. D. Myers and W. J. Świątecki, “Thomas-Fermi fission barriers,” *Phys. Rev. C* **60**, 014606 (1999).
- [38] We stress that the BCPM β -delayed fission rates are based on β -strength functions, and hence Q_β values, predicted by FRDM. For consistency the lower middle panel of Fig. 1 shows the difference between the BCPM fission barriers and FRDM Q_β values, since the latter were used to determine the maximum β -decay energy.
- [39] Andreas Bauswein, Stéphane Goriely, and Hans-Thomas Janka, “Systematics of Dynamical Mass Ejection, Nucleosynthesis, and Radioactively Powered Electromagnetic Signals From Neutron-Star Mergers,” *Astrophys. J.* **773**, 78 (2013).
- [40] Jonas Lippuner and Luke F. Roberts, “r-Process Lanthanide Production and Heating Rates in Kilonovae,” *Astrophys. J.* **815**, 82 (2015).
- [41] Rodrigo Fernández and Brian D. Metzger, “Delayed outflows from black hole accretion tori following neutron star

- binary coalescence,” *Mon. Notices Royal Astron. Soc.* **435**, 502–517 (2013).
- [42] O. Just, A. Bauswein, R. Ardevol Pulpillo, S. Goriely, and H.-T. Janka, “Comprehensive nucleosynthesis analysis for ejecta of compact binary mergers,” *Mon. Notices Royal Astron. Soc.* **448**, 541–567 (2015).
- [43] D. M. Siegel and B. D. Metzger, “Three-Dimensional General-Relativistic Magnetohydrodynamic Simulations of Remnant Accretion Disks from Neutron Star Mergers: Outflows and r-Process Nucleosynthesis,” *Phys. Rev. Lett.* **119**, 231102 (2017).
- [44] L. Phillips, R.C. Gatti, R. Brandt, and S.G. Thompson, “Spontaneous fission half lives of ^{254}Cf , ^{255}Fm , and ^{250}Cf ,” *J. Inorg. Nucl. Chem.* **25**, 1085–1087 (1963).